ISSN 2435-5453

Technical Journal of Advanced Mobility

次世代移動体技術誌

論　文

JUIDA
Japan UAS Industrial Development Association

Vol. 7
2026

Development of CO_2 Gas Sensing Method using Formation Flight with Four Drones

Shanfeng Zhang[*1], Shigenori Togashi[*2], Etsuki Yoshimura[*2]
Graduate School of Advanced Science and Engineering, Waseda University[*1]
Mechanical Engineering Course, School of Science and Engineering, Kokushikan University[*2]

Understanding gas concentration distributions near the ground is important for disaster prevention and safety management. In this study, as part of expanding drone applications, we tried to develop the CO_2 gas sensing method using formation flight with four drones. By flow simulation, we confirmed the gas updraft flow not only velocity but also concentration distribution generated by the drones. It was confirmed that the updraft flow velocity around the sensor was 2 m/s at the height of 0.3 m, and the concentration ratio was between 0.95 and 0.99, respectively. Then, to stable the formation flight with four drones, a rope was used between the connecting rod and the drone. Then, the CO_2 sensing experiment using this approach was conducted. The average concentration values of 4,290 and 4,710 ppm of three experiments were measured at the heights of 0.5 m and 0.3 m, respectively. Moreover, we tried to predict the concentration at the CO_2 source using the steady-state one-dimensional convection-diffusion equation. It was found that the predicted concentration of 4,772 ppm at the CO_2 source was in between 4,700 and 4,800 ppm measured by sensor. Finally, the effectiveness of prediction was confirmed.

Keywords: Drone, Formation flight, Flow simulation, Gas sensing, Convection, Diffusion, Prediction

1. Introduction

There is a wide range of possible applications for drones, such as for infrastructure inspection, agriculture, logistics, photography, disaster prevention, and gas sensing. In dangerous site inspection, their ability to quickly collect information in hazardous areas where human entry is dangerous has become increasingly important. The poisonous hydrogen sulfide (H_2S) gas and high concentration CO_2 gas, being heavier than air, tend to accumulate near the ground in underground or enclosed spaces, potentially causing delayed responses, oxygen deficiency, or poisoning. Understanding gas concentration distributions in such environments is important for disaster prevention and safety management. In recent years, papers have been published on the use of drones for gas sensing tasks. Li, et al. [1] reported the air quality monitoring, and Motlagh, et al. [2] reported the air pollution monitoring using a drone in flight, respectively. On the other hand, Neumann, et al. [3] reported results of gas source localization experiments using a drone equipped with several different types of gas sensors by applying a particle filter-based algorithm to the sensor data collected in flight. Successful gas source localization demonstrations were also reported for a drone equipped with a laser-based remote methane detector [4]. Despite these successful examples, there is a problem using drone for gas sensing tasks. The rotors of a drone produce a strong downwash to obtain the lift force. Most gas sensors show a response only when a gaseous chemical substance touches the sensor surface. The gas contained in the surrounding air needs to be transported to the sensor surface by convection and diffusion. When a drone flies, the downwash generated by rotors blows off the gas near the ground. This problem has been raised even in early work on gas sensing drones [5]. To solve the above problem, Sato, et al. [6] proposed the gas sensing method by using the fountain flow [7]

generated by the two drones connected by a rod. In their paper, the flow velocity distribution by numerical simulation and the experimental results with air were also reported. Moreover, Akaogi, et al. [8] proposed the gas sensing method by using the fountain flow generated by the extended arm quad type drone. In their paper, their experimental results with ethanol gas were also reported.

In the above previous studies, there are still some issues as follows. First, the gas updraft flow velocity distribution generated by the drones is shown using flow simulation, but the gas concentration distribution is not shown. Second, the formation flight equipped with the gas sensor is unstable in case of direct connection between rods and each drone. Third, there was no prediction of CO_2 concentration at the source based on the sensing point.

Therefore, in this study, we assumed the application example of CO_2 sensing with heavier than air and larger amount at the underground parking lot as shown in **Fig.1**. First, flow simulation was conducted to visualize the gas updraft flow not only flow velocity but also concentration distribution generated by the drones as detailed in Chapter 2. Second, the formation flight equipped with the gas sensor is unstable in case of direct connection between rods and each drone. Therefore, a rope was used between the connecting rod and the drone, instead of connecting the rod directly to the drone. With this approach, the individual differences of drone position and height were compensated for by the rope, and the formation flight with four drones were stably continued as detailed in Chapters 3 and 4. Third, we conducted CO_2 sensing experiments using formation flight with four drones and predicted CO_2 concentration at the source from the sensing points using the one-dimensional convection-diffusion equation as detailed in Chapters 5, 6, and 7.

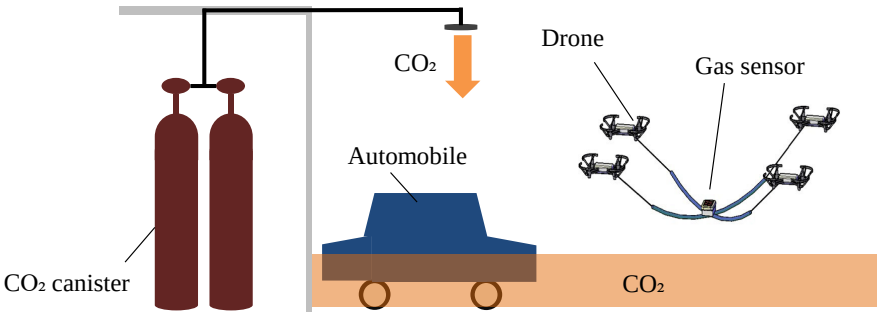

Fig.1 Application example of CO_2 sensing at the underground parking lot.

2. Flow simulation

To visualize the gas updraft flow not only flow velocity but also concentration distribution generated with the drones, flow simulation was conducted using the software Flowsquare$^+$ [9-11]. The gas concentration transport equation is also solved with the momentum transport equation in Flowsquare$^+$, and the application example papers have been published [12,13]. **Figure 2** shows the flow simulation domain and boundary conditions of flow simulation around two drones. Parameters lx, ly, lz, nx, ny, and nz represent Length in x, y, z direction, number of grids in x, y, and z direction, respectively. **Table 1** is specification of parameters using the boundary conditions of flow simulation. Here, the domain in the z direction was thinned to perform quasi-two-dimensional simulation. Parameters W_d, P_d, and H_d represent the width of drone, the diameter of drone propeller, and hovering height, respectively. Flow simulation conducted both one drone and two drones. In case of two drones, L represents the distance between drones as shown in **Fig.2**. Parameters VinG and VinR are the inflow velocity at the top of drone propeller (Boundary color: Green) and the outflow velocity at the bottom of drone propeller (Boundary color: Red) measured with a Pitot tube and set to 8 m/s as the velocity boundary condition of drone

1. Similar boundary conditions were also set for drone 2. Parameters W_s, H_s, and D_s represent the width of sensor housing, installation height of sensor housing, and thickness of sensor housing, respectively. Here, the sensor housing was set only in case of simulation for two drones.

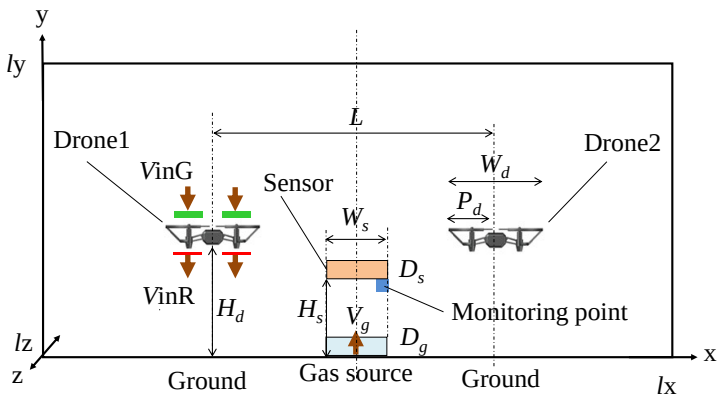

Fig.2 Flow simulation domain and boundary conditions.

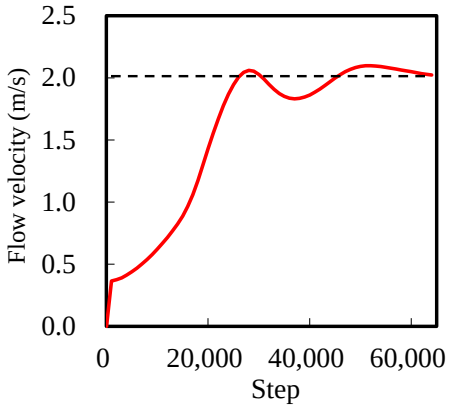

Fig.3 Flow velocity convergence at the monitoring point.

Table 1 Specification of parameters using the boundary conditions of flow simulation.

No.	Parameters	Explanation of parameters	Input data	
			One drone	Two drones
1	*lx*	Length in x direction (m)	2.5	2.5
2	*ly*	Length in y direction (m)	1.0	1.0
3	*lz*	Length in z direction (m)	0.05	0.05
4	*nx*	Number of grids in x direction	250	250
5	*ny*	Number of grids in y direction	100	100
6	*nz*	Number of grids in z direction	5	5
7	W_d	Width of drone (m)	0.20	0.20
8	P_d	Diameter of drone propeller (m)	0.08	0.08
9	H_d	Hovering height (m)	0.4	0.4
10	L	Distance between drones (m)	-	1.5
11	*V*inG	Inflow velocity at the top of drone propeller (Boundary color: Green)	-8.0	-8.0
12	*V*inR	Outflow velocity at the bottom of drone propeller (Boundary color: Red)	-8.0	-8.0
13	W_s	Width of sensor housing (m)	-	0.2
14	H_s	Installation height of sensor housing (m)	-	0.3
15	D_s	Thickness of sensor housing (m)	-	0.05
16	D_g	Thickness of gas ejection source (m)	-	0.05
17	V_g	Gas ejection velocity (m/s)	0.1	0.1
18	C_g	Gas concentration ratio	1.0	1.0
19	*mu*	Air viscosity coefficient (Pa·s)	1.8×10^{-5}	1.8×10^{-5}
20	C_s	Coefficient of Smagorinsky turbulence model	0.17	0.17
21	*cfl*	Courant-Friedrichs-Lewy number	0.01	0.01

Parameters D_g, V_g, and C_g represent the thickness of gas ejection source, gas ejection velocity, and gas concentration ratio, respectively. Last parameters *mu*, C_s, and *cfl* represent air viscosity coefficient, the coefficient of Smagorinsky turbulence model [14,15], and Courant-Friedrichs-Lewy number, respectively. For stable flow simulation, the Courant number (CFL) number for the explicit method was set to a small value of 0.01. **Figure 3** shows the state of flow velocity convergence at the monitoring point near the sensor in **Fig.2**. It was confirmed that the flow velocity at the monitoring point converged to approximately 2.0 m/s after 63,000 simulation steps.

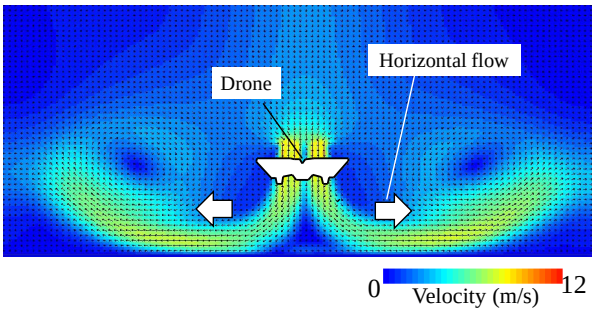

(a) Flow velocity distribution

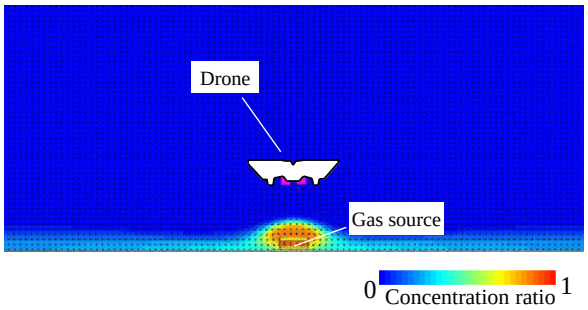

(b) Concentration distribution

Fig.4 Flow simulation results in case of one drone.

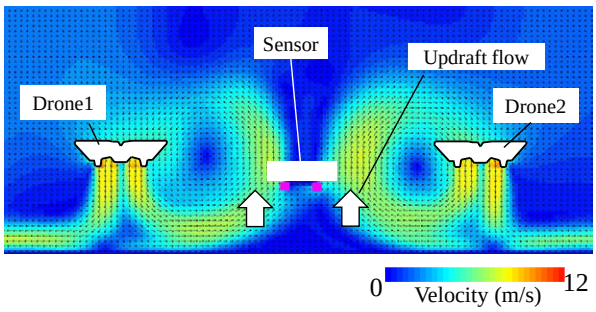

(a) Flow velocity distribution

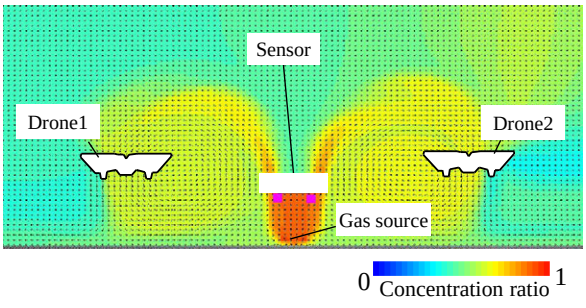

(b) Concentration distribution

Fig.5 Flow simulation results in case of two drones.

Figure 4 shows the flow simulation results in case of one drone. **Figures 4(a)** and **4(b)** are the flow velocity and concentration distribution, respectively. The downwash flow generated by the drone spread out as the horizontal flow along the ground after reaching the ground as shown in **Fig.4(a)**. Therefore, it has been confirmed that the concentration distribution from the gas source became horizontally as shown in **Fig.4(b)**. Here, the concentration distribution is expressed as the normalized concentration ratio and ranges from 0 to 1.

Figure 5 shows the flow simulation results in case of two drones. **Figures 5(a)** and **5(b)** are the flow velocity and concentration distribution, respectively. The downwash flow generated by two drones rolled up as the updraft flow after reaching the ground. Therefore, it has been confirmed that the concentration from the gas source became updraft flow and reached the sensor shown in **Fig.5(b)**. Moreover, it was confirmed that the concentration ratio around the sensor was between 0.95 and 0.99.

3. CO_2 gas sensor

For the formation flight with four drones, the requirements of CO_2 gas sensor are lightweight (100 g or less) and wireless communication function. As a sensor with satisfying the above requirements, we selected the RICOH EH CO_2 sensor D101 [16] as shown in **Fig.6**. **Figures 6(a)** and **6(b)** show the surface side with wireless communication using the solar panel and the protective housing, and reverse side with four intake ports (No.1-4) and two exhaust ports (No.5,6). **Figure 6(c)** shows the inner configuration using NDIR (Non Dispersive IfraRed)-type. The CO_2 concentration was calculated from Eq. (1).

$$T = \frac{I}{I_0} = e^{-\varepsilon C d} \tag{1}$$

where T, I, I_0, ε, C, and d represent transmittance, intensity of transmitted light, intensity of incident light, absorbance, CO_2 concentration, and optical path length, respectively.

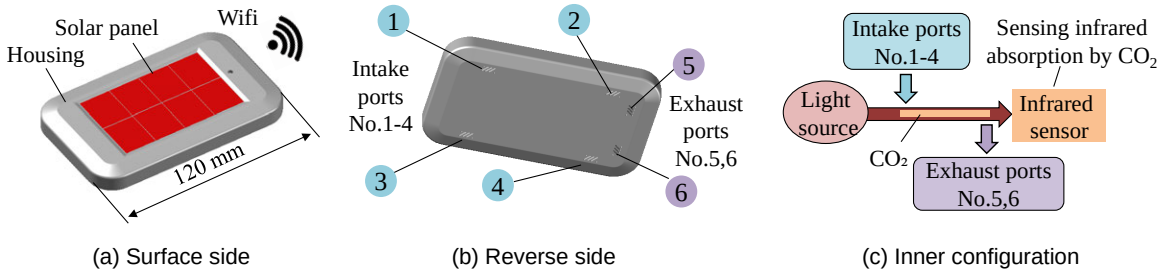

(a) Surface side　(b) Reverse side　(c) Inner configuration

Fig.6 Schematic of CO_2 sensor module and inner configuration.

4. Design of formation flight configuration

Figure 7 shows a schematic of formation flight configuration with four drones and the control method. The drone used was a Tello EDU with specifications listed in **Table 2**. The four drones were simultaneously controlled by a single personal computer using Python program. A rope was used between the connecting rod and the drone with a spacing of 1.3 m, instead of connecting the rod directly to the drone [17,18] as shown in **Fig.7**. With this approach, the individual differences of drone position and height were compensated for by the rope, and the formation flight with four drones were stably continued. The CO_2 sensor was suspended at the center of a four-drone square formation and the concentration data were sampled at 10 second intervals in the tablet computer by wireless communication function.as shown in **Fig.7**. The payload of a Tello EUD is 30 g as shown in **Table 2**. Therefore, the total payload of the formation flight with four drones becomes 120 g, and the total components weight was 111 g less than the required 120 g with the weight breakdown of components listed in **Table 3**.

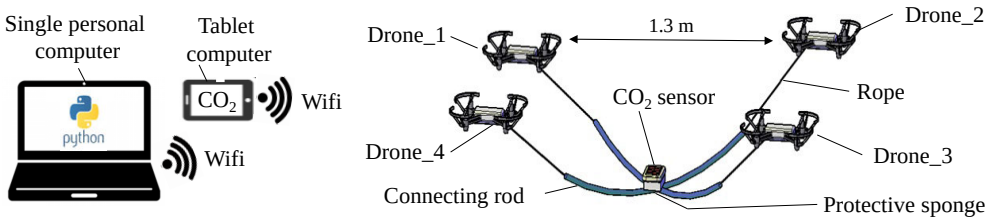

Fig.7 Schematic of formation flight configuration with four drones and the control method.

Table 2 Specifications of a drone.

Drone	Tello EDU
Payload of a drone (g)	30
Weight (g)	87
Maximum flight time (min)	13
Number of formation flights	4

Table 3 Weight breakdown of components.

Component	Number	Weight [g]
Connecting rod	4	16
Protective sponge	1	1
CO_2 sensor	1	90
Rope	4	4
Total weight (g)	-	111 < 120

5. CO_2 gas sensing experiment at the fixed position

Figure 8 shows a schematic of CO_2 sensing experiment at the fixed position. The CO_2 gas was generated by placing 400 g of dry ice in 300 g of water (mass ratio 4:3) into a plastic container with the size of 220 × 170 × 50 mm as the CO_2 gas source. The CO_2 gas source concentration was measured to be between 2,200 and 2,300 ppm by sensor. The four-drone formation hovered so that the height of CO_2 sensor kept 0.3 m, and the plastic container of CO_2 gas source was in at 5 seconds and out at 90 seconds under the four-drone formation as shown in **Fig.8**.

The initial indoor concentration was approximately 1,000 ppm. **Figure 9** shows the sensing results of CO_2 concentration for 160 seconds. When the four-drone formation was fixed in hovering mode directly above the dry ice source at a height of 0.3 m. In 5 seconds, the plastic container of CO_2 gas source was in under the four-drone formation. In 55 seconds, the maximum concentration of 2,100 ppm was observed corresponding to an increase of approximately 1,100 ppm over the background concentration. Moreover, in 90 seconds, the plastic container of CO_2 gas source was out, and in 160 seconds, CO_2 concentration returned to initial value as shown in **Fig.9**.

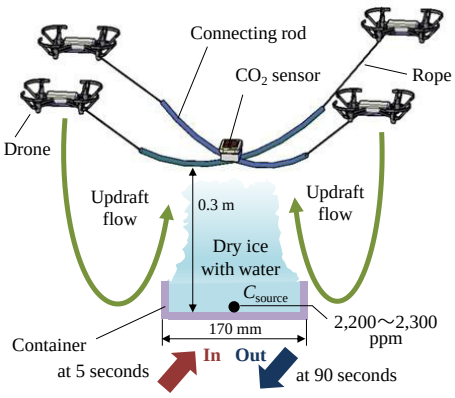

Fig.8 Schematic of CO_2 sensing experiment at the fixed position.

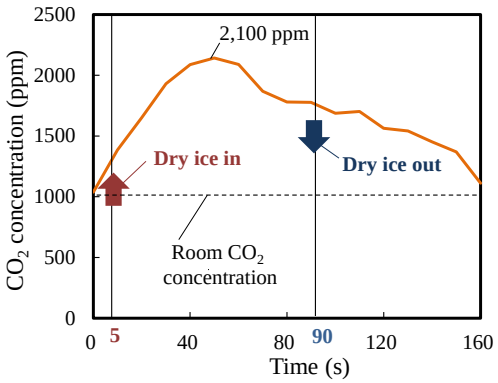

Fig.9 Sensing results of CO_2 concentration.

6. CO_2 gas sensing experiment with the horizontal flight

Figure 10 shows a schematic of CO_2 sensing experiment with the horizontal flight. The CO_2 gas was generated by placing 1,600 g of dry ice in 1,200 g of water (mass ratio 4:3) into four plastic containers with the size of $220 \times 170 \times 50$ mm as the CO_2 gas source. The CO_2 gas source concentration was measured to be between 4,700 and 4,800 ppm by sensor as shown in **Fig.10**.

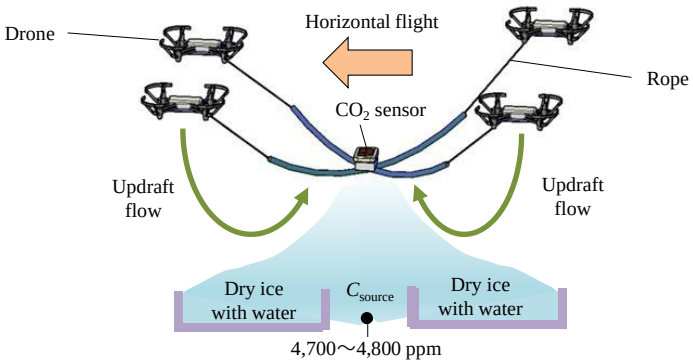

Fig.10 Schematic of experiment with the horizontal flight.

The experiment was conducted three times, and the amount of dry ice decreased over time. Therefore, dry ice was added as needed to ensure the concentration was within the range of 4,700 to 4,800 ppm before the experiment was conducted. Additionally, experiments were conducted at two heights of 0.3 m and 0.5 m. By using Python-based automatic flight control, a flight sequence consisting of takeoff, horizontal movement, hovering for 10 seconds above the CO_2 source, retreat, and landing. The influence of horizontal movement on

the updraft flow behavior of the formation was evaluated.

Figure 11 shows photographs of CO_2 sensing experiment with the horizontal flight. **Figure 11(a)** shows flight at the height of 0.5 m, and **Figure 11(b)** shows flight at the height of 0.3 m. **Figure 12** shows sensing results of the CO_2 concentration **Figure 12(a)** shows the CO_2 concentration at the height of 0.5 m, and it was confirmed that the concentration increased to a maximum of 4,230 ppm. **Figure 12(b)** shows the CO_2 concentration at the height of 0.3 m, and it was confirmed that the concentration increased to a maximum of 4,673 ppm. Additionally, the prediction of CO_2 concentration at the source based on the two sensing points is conducted in next Chapter 7.

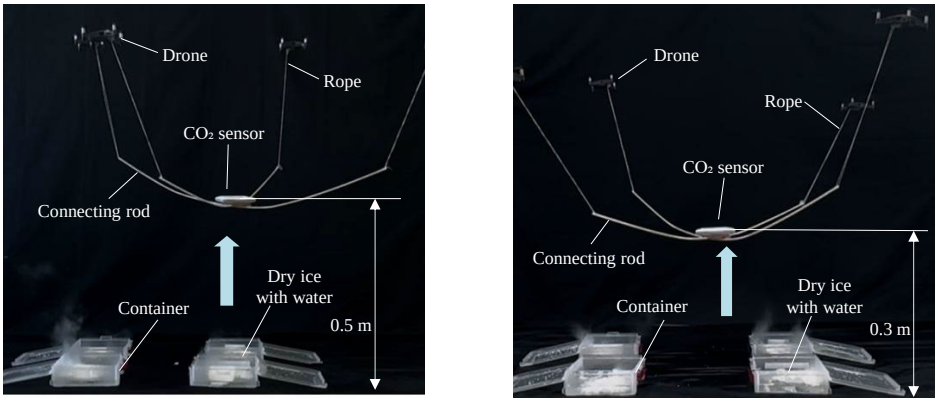

(a) Flight at the height of 0.5 m　　(b) Flight at the height of 0.3 m

Fig.11 Photographs of CO_2 sensing experiment with the horizontal flight at the hovering for 10 seconds.

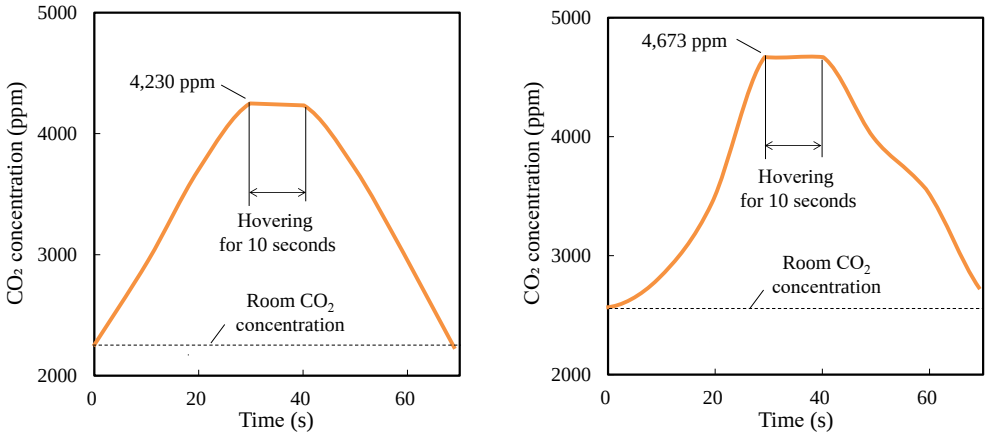

(a) Flight at the height of 0.5 m　　(b) Flight at the height of 0.3 m

Fig.12 Sensing results of CO_2 concentration.

7. Prediction of CO_2 concentration at the source

To predict CO_2 concentration at the source based on the two sensing points at the heights of 0.5 m and 0.3 m, the steady-state one-dimensional convection-diffusion equation [19] is used as shown in Eq. (2).

$$u\frac{dC}{dz} = D_t\frac{d^2C}{dz^2} \tag{2}$$

where C, u, z, and D_t represent concentration, velocity, vertical coordinates, and turbulent diffusion coefficient, respectively. Equation (2) has the exact solution with the boundary condition: $C = C_0$ at $z = 0$, $C = C_H$ at $z = H$ as

shown in Eq. (3).

$$C(z) = C_0 + \frac{e^{Pe\frac{z}{H}} - 1}{e^{Pe} - 1}(C_H - C_0) \tag{3}$$

Here, Pe is Peclet number defined as Eq. (4) using turbulent diffusion coefficient D_t.

$$Pe = \frac{uH}{D_t} \tag{4}$$

Table 4 shows the values for calculation of Peclet number Pe, we used CO_2 molecular diffusion coefficient $D_m = 1.64 \times 10^{-5}$ m^2/s [20], and ratio of turbulent to molecular diffusion coefficient $D_t / D_m = 10^4$ (Average of 10^3–10^5) [21].

Table 4 Values for calculation of Peclet number Pe.

CO_2 molecular diffusion coefficient [20] D_m (m^2/s)	Ratio of turbulent to molecular diffusion coefficient [21] D_t / D_m	Velocity u (m/s)	Height H (m)
1.64×10^{-5}	10^4 (Average of $10^3 - 10^5$)	2.0	0.5

Table 5 shows the predicted result of concentration at the CO_2 source. The average concentration values of 4,290 and 4,710 ppm of three experiments ($N = 3$) were used at the heights of 0.5 m and 0.3 m, respectively. By substituting these average concentrations into Eqs. (3) and (4), the concentration at the CO_2 source was predicted as 4,772 ppm. Additionally, it was found that the predicted concentration of 4,772 ppm at the CO_2 source was in between 4,700 and 4,800 ppm measured by sensor as shown in Fig.12. Finally, the effectiveness of prediction was confirmed.

Table 5 Predicted result of concentration at the CO_2 source in case of horizontal fight experiment (Fig.12).

Height (m)	Concentration (ppm)	Method
0.5	4,290	Experimental average $N = 3$
0.3	4,710	Experimental average $N = 3$
0.0 (CO_2 source)	4,772	Using Eqs. (3) and (4)

8. Discussion

It is necessary for gas sensing using drones to consider the drone down's wash flow. Therefore, there are four categories based on the amount of gas generation and the specific gravity relative to air. First category is the gas lighter than air and small amount. Second category is the gas lighter than air and large amount. Third category is the gas heavier than air and small amount. Fourth category is the gas heavier than air and large amount. Here, the determination whether to the large or small amount is based on the following criteria, that is, the large amount is defined as that the stable gas supply is larger than the blowing away by the drone's downwash.

This study belongs to fourth category, and we need to generate the updraft flow for sensing the gas heavier than air and large amount. In contrast, in case of first and third categories, the sensor must be suspended using a sufficiently long rope to avoid the influence of the flying drone's downwash. Additionally, in case of second category, the regular drone equipped with sensor can land on the gas source and sense the gas because the gas

is lighter than air and large amount. To conduct the study in the above categories, it is necessary to solve the distance reached by the drone's downwash using flow simulation. We have already conducted the above study and plan to report in next paper.

9. Conclusion

In this study, as part of expanding drone applications, we tried to develop the CO_2 gas sensing method using formation flight with four drones. Flow simulation of the gas updraft flow, the construction of formation flight, CO_2 sensing experiments, and prediction of CO_2 concentration at the source were conducted. The following conclusions were obtained.

(1) By flow simulation, we confirmed the gas updraft flow not only velocity but also concentration distribution generated by the drones. It was confirmed that the updraft flow velocity around the sensor was 2 m/s at the height of 0.3 m, and the concentration ratio was between 0.95 and 0.99, respectively.
(2) A rope was used between the connecting rod and the drone, instead of connecting the rod directly to the drone. With this approach, the individual differences of drone position and height were compensated for by the rope, and the formation flight with four drones were stably continued. Then, the CO_2 sensing experiment using this approach was conducted. The average concentration values of 4,290 and 4,710 ppm of three experiments were measured at the heights of 0.5 m and 0.3 m, respectively.
(3) Moreover, prediction of the concentration at the CO_2 source was conducted using the steady-state one-dimensional convection-diffusion equation. It was found that the predicted concentration of 4,772 ppm at the CO_2 source was in between 4,700 and 4,800 ppm measured by sensor. Finally, the effectiveness of prediction was confirmed.

Received: December 8, 2025
Accepted: January 7, 2026

References

[1] Li, Y., Huang, Y. and Chen, S.: "Air Quality Detection Drone System Based on Beidou Navigation System," *Computer Science and Application*, Vol. 9, No. 4, Article ID: 29659, pp. 703–709, 2019.
[2] Motlagh, N.H., Kortoçi, P., Su, X. and Lovén, L.: "Unmanned Aerial Vehicles for Air Pollution Monitoring: A Survey," *IEEE Internet of Things Journal*, Vol. 10, No. 24, pp. 21687–21704, 2023.
[3] Neumann, P.P., Hernandez Bennetts, V., Lilienthal, A.J., Bartholmai, M. and Schiller, J.H.: "Gas source localization with a micro-drone using bio-inspired and particle filter-based algorithms," *Adv. Robot.*, Vol. 27, pp. 725–738, 2012.
[4] Golston, L.M., Aubut, N.F., Frish, M.B., Yang, S., Talbot, R.W., Gretencord, C., McSpiritt, J. and Zondlo, M.A.: "Natural gas fugitive leak detection using an unmanned aerial vehicle: Localization and quantification of emission rate," *Atmosphere*, Vol. 9, No. 333. pp. 1–17, 2018.
[5] Neumann, P.P., Asadi, S., Lilienthal, A.J., Bartholmai, M. and Schiller, J.H.: "Autonomous gas-sensitive microdrone: Wind vector estimation and gas distribution mapping," *IEEE Robot. Autom. Mag.*, Vol. 19, pp. 50–61, 2012.
[6] Sato, R., Tanaka, K., Ishida, H., Koguchi, S., Ramirez., J. P. R., Matsukura, H. and Ishida, H.: "Detection of Gas Drifting Near the Ground by Drone Hovering Over: Using Airflow Generated by Two Connected Quadcopters," *Sensors*, Vol. 20, No. 5, pp. 1–16, 2020.
[7] Li, Q., Page, G.J. and McGuirk, J.J.: "Large-eddy simulation of twin impinging jets in cross-flow," *Aeronaut. J.* Vol. 111, pp.195–206, 2007.
[8] Akaogi, D., Yamashita, K., Matsukura, H., and Ishida, H.: "Development of Gas Sensing Drone: Influence of Tilted Ground on

Gas Transport," *Proc. of The Japan Society of Mechanical Engineers*, S115-05, 2021.
[9] Minamoto, Y.: "Numerical Thermo-Fluid Dynamics with Fluid Simulation Software Course Flowsquare$^+$(1)," *Journal of Mechanical Research*, Vol. 72, No. 9, pp. 677–681, 2020.
[10] Trájer, A. J.: "Ecological evaluation of the development of Neanderthal niche exploitation," *Quaternary Science Reviews*, Vol. 310, 108127, 2023.
[11] Tajima, Y., Hiraguri, T., Matsuda, T., Imai, T., Hirokawa, J., Shimizu, H., Kimura, T. and Maruta, K.: "Analysis of Wind Effect on Drone Relay Communications," *Drones* Vol. 7, No. 3, 182, https://doi.org/10.3390/drones7030182, 2023.
[12] Togashi, S., Zhang, H. and Miyake, R.: "Development of a measuring system for the volatilization characteristics of essential oils and evaluation of the measured data by advection–diffusion simulation," *Japan Journal of Aromatherapy*, Vol. 26, No. 1, pp. 1–9, 2025.
[13] Ishigaki, Y., Kawauchi, Y., Yokogawa, S., Saito, A., Kitamura, H. and Moritake, T.: "Ventilatory effects of excessive plastic sheeting on the formation of SARS-Cov-2 in a closed indoor environment," *Environmental and Occupational Health Practice*, 5: eohp.2022-0024-OA, pp. 1–9, 2023.
[14] Koyama, S.: "Large eddy simulation of the turbulent pipe flow using dynamic subgrid-scale model," *Institute of Industrial Science*, Vol. 57, No. 1, pp. 58–62, 2005.
[15] Fujiwara, S.: "Experimental Study on Synchronized Swimming in the Kármán Vortex Behind an Object Using a Fish Robot," *Journal of Aero Aqua Bio-mechanisms*, Vol. 11, No. 1, pp. 10–17, 2025.
[16] Takeuchi, K.: "Current status and future of energy harvesting technologies," *Journal of the Japan Society for Precision Engineering*, Vol. 88, No. 11, pp. 805–808, 2022.
[17] Ando, T. and Togashi, S.: "Flight Stability Analysis of Formation Drones and Application to Netting Operation," *Technical Journal of Advanced Mobility*, Vol. 6, No. 8, pp. 57–66, 2025.
[18] Ando, T., Aoki, H. and Togashi, S.: "Flight Stabilization of Drones near Ceiling and Its Application to Cabling," *Proc. of the 30th Annual Meeting of Kanto Branch*, JSME, 14G02, 2024.
[19] Ferziger, J. and Peric, M.: Computational method for fluid dynamics, 3rd Edition, Springer, pp. 76–83, 2002.
[20] Matsunaga, N., Hori, M. and Nagashima, A.: "5th Report Measurements of the mutual diffusion coefficients of gases by the Taylor method," *Transactions of the Japan Society of Mechanical Engineers.* Part B, Vol. 64; No. 621, pp. 149–155, 1998.
[21] Levenspiel, O.: Chemical Reaction Engineering, 3rd ed., John Wiley & Suns, p. 311, 1999.

張　山峰
2025 年 3 月国士舘大学理工学部機械工学系卒業。富樫研究室に所属時に編隊飛行する 4 台のドローンによる CO_2 検知法を開発し，Technical Journal of Advanced Mobility ポスターセッション in Japan Drone 2025 に発表。2025 年 4 月早稲田大学大学院生命理工専攻に進学。現在，介護分野へのセンシング技術の応用拡大に取り組んでいる。
E-mail：zsf@akane.waseda.ac.jp

吉村　越輝
2022 年 4 月 国士舘大学理工学部機械工学系入学。富樫研究室に所属。流体力学的観点からドローンの適用拡大の研究を推進中。主に，ドローンによる CO_2 検知法，飛行しているドローンからの流体音による状態診断の開発に取り組んでいる。
E-mail：s23a362b@kokushikan.ac.jp

富樫　盛典
1995 年 3 月 東京大学大学院工学系研究科機械工学専攻博士課程修了，博士（工学）。1995 年 4 月（株）日立製作所機械研究所に入社。研究室長，主管研究員を歴任。日本機械学会フェロー，日本流体力学会フェロー。2020 年 4 月より国士舘大学理工学部機械工学系の教授として着任。流体力学的観点からドローンの適用拡大の研究を推進中。JUIDA 無人航空機操縦士，一等無人航空機操縦士（国家資格）。
E-mail：togashis@kokushikan.ac.jp

一般社団法人 日本 UAS 産業振興協議会（JUIDA）

JUIDA は、日本の無人航空機システム（UAS）の、民生分野における積極的な利活用を推進し、UAS 関係の新たな産業・市場の創造を行うとともに、UAS の健全な発展に寄与することを目的とした中立、非営利法人として、2014 年 7 月に設立されました。

国内外の研究機関、団体、関係企業と広く連携を図り、UAS に関する最新情報を提供するとともに、さまざまな民生分野に最適な UAS を開発できるような支援を行っています。同時に、UAS が安全で、社会的に許容されうる利用を実現するために、操縦技術、機体技術、管理体制、運用ルール等の研究を行うとともに政策提言を行っています。

Technical Journal of Advanced Mobility
次世代移動体技術誌

第 7 号

発行日　：2026 年 1 月 20 日
編集・発行　：一般社団法人日本 UAS 産業振興協議会
東京都文京区本郷 5-33-10
いちご本郷ビル 4F
URL　：https://uas-japan.org/
email　：journal@uas-japan.org

ISSN　2435-5453